RESEARCH ARTICLE | JUNE 02 1997

Thermal conductivity of Si–Ge superlattices

S.-M. Lee; David G. Cahill; Rama Venkatasubramanian

Appl. Phys. Lett. 70, 2957–2959 (1997)
https://doi.org/10.1063/1.118755

Thermal conductivity of Si–Ge superlattices

S.-M. Lee and David G. Cahill[a)]
Department of Materials Science and Engineering and the Coordinated Science Laboratory, University of Illinois, Urbana, Illinois 61801

Rama Venkatasubramanian
Center for Semiconductor Research, Research Triangle Institute, Research Triangle Park, Durham, North Carolina 27709-2195

(Received 10 February 1997; accepted for publication 3 April 1997)

The thermal conductivity of Si–Ge superlattices with superlattice periods $30<L<300$ Å, and a $Si_{0.85}Ge_{0.15}$ thin film alloy is measured using the 3ω method. The alloy film shows a conductivity comparable to bulk SiGe alloys while the superlattice samples have a thermal conductivity that is smaller than the alloy. For $30<L<70$ Å, the thermal conductivity decreases with decreasing L; these data provide a lower limit to the interface thermal conductance G of epitaxial Si–Ge interfaces: $G>2\times10^9$ W m^{-2} K^{-1} at 200 K. Superlattices with relatively longer periods, $L>130$ Å, have smaller thermal conductivities than the short-period samples. This unexpected result is attributed to a strong disruption of the lattice vibrations by extended defects produced during lattice-mismatched growth. © *1997 American Institute of Physics.* [S0003-6951(97)03922-3]

The epitaxial growth of thin films allows scientists and engineers to produce superlattice materials with unique physical properties. The electronic and optoelectronic properties of superlattices have been widely studied. Recently, the *thermal* properties of quantum wells[1] and superlattices[2] have come under intense investigation because of the promise of demonstrating greatly improved figure-of-merits for thermoelectric cooling and power conversion, and because heat transport in optoelectronic devices is severely degraded by a large density of epitaxial interfaces.[3]

(GaAs)–(AlAs) superlattices have been the topic of several studies of superlattice thermal conductivity[4–7] and phonon transport.[8,9] These experiments have shown that the room temperature thermal conductivity measured in the in-plane direction decreases with decreasing superlattice period[4] and that a stronger reduction is produced in the through-thickness direction.[5,7] Since the lattice mismatch between GaAs and AlAs is extremely small, superlattices of any period can be grown with excellent crystal quality. Differences in the density and elastic constants, however, are also small; we can expect that the relatively small ''acoustic-mismatch'' between GaAs and AlAs limits the strength of interface effects in thermal transport.[10]

In this work, we report our experimental study of the thermal conductivity of Si–Ge superlattices. The differences in vibrational spectra of Si and Ge are much larger than for GaAs and AlAs, and our measurements, discussed below, show that the thermal conductivities of short-period Si–Ge superlattices are indeed smaller than comparable (AlAs)-(GaAs) superlattices. [Since AlAs, GaAs, Si, and Ge all have similar bond lengths, we can simply compare the differences in sound velocity: For (AlAs)–(GaAs), the ratio of sound velocities is ≈1.2; for Si–Ge, the ratio of the sound velocities is ≈1.7.] Longer period Si–Ge superlattices show a surprisingly small thermal conductivity that approaches the behavior typical of highly disordered solids.[11]

Si–Ge superlattices and SiGe alloy films are grown on semi-insulating GaAs substrates at 750 °C from silane and germane precursors. Prior to superlattice growth, a 1 μm-thick Ge buffer layer is deposited; Ge is lattice-matched to GaAs. The total thickness of the Si–Ge layers ranges from 0.9 to 1.8 μm as measured by scanning electron microscopy of the sample cross section. We determine the superlattice period from the total Si–Ge layer thickness divided by the number of growth cycles (silane deposition followed by germane deposition). We use Rutherford backscattering spectroscopy (RBS) to measure the average composition of the films. If we assume that each layer is either pure Ge or pure Si, the RBS data also yield the thicknesses of the Si and Ge layers that make up the superlattice (see Table I). High-resolution x-ray diffraction (XRD) shows that the average lattice constant of the short-period superlattices is approximately equal to the lattice constant of a bulk alloy with the same average composition.

The SiGe films are *n* type, with As doping levels in the range $3–20\times10^{18}$ cm^{-3} measured on separate samples. The exact carrier concentration of the thermal conductivity samples is unknown. For bulk SiGe alloys at $T=300$ K, increasing the *n*-type carrier concentration from 3×10^{18} to 2×10^{19} cm^{-3} produces an additional thermal resistivity of

TABLE I. Description of the Si_m–Ge_n superlattices and SiGe alloy film measured in this study. The thickness of each Si and Ge layer is approximate and given in units of the monolayer thickness 1.38 Å.

Sample No.	$m\times n$ (monolayers)	Superlattice period (Å)	Film thickness (μm)
139	146×54	275	1.65
142	0.85:0.15 (*alloy*)	—	1.14
143	74×34	150	1.2
144	72×30	140	1.4
149	35×9	60	1.8
153	13×9	30	0.9
154	23×13	50	1.5
155	19×5	33	1.0
191	22×25	65	1.3

a)Electronic mail: d-cahill@uiuc.edu

3 cm K W^{-1}.[12] Assuming that charge carriers in Si–Ge superlattices produce a similar thermal resistance, we estimate that the uncertainty in the doping level creates an uncertainty of less than $\pm 10\%$ in our thermal conductivity data.

We measure the film thermal conductivity using the 3ω method.[13] Since the superlattice samples are electrically conducting, we cannot simply place the heater-thermometer pattern on the surface of the samples; for electrical insulation, we first deposit a $\sim$100 nm SiO_2 film using plasma enhanced chemical vapor deposition (PECVD) at 300 °C. Then, the heater-thermometer line is produced by evaporating a $\sim$300-nm-thick gold heater film, with a $\sim$4 nm chromium adhesion layer, followed by patterning using the lift-off method. The Au heater-thermometer line is 0.5 mm long and 8 μm wide. Data are collected over a wide frequency range; typically the data near 1 kHz are used in the data analysis. The measurement gives the series thermal conductance of the dielectric layer and the superlattice sample; the contribution from the dielectric layer is measured separately and subtracted from the raw data.[14] (Since we expect the 1-μm-thick Ge buffer layer to have a large thermal conductivity nearly identical to bulk Ge—and therefore also close to the conductivity of the GaAs substrate—we do not need to consider the thermal conductance of the buffer layer in our data analysis.) A detailed description of the measurement method and data analysis is given in Refs. 13 and 14.

To confirm the reliability of our measurements, we compare the thermal conductivity of a 1-μm-thick SiGe alloy film to the thermal conductivity of a bulk SiGe alloy[15] (see Fig. 1). We see that the bulk and thin film alloy have, as expected, essentially the same conductivity. Data for the pure crystals[14,16] and the amorphous phases[13,17] are included in Fig. 1 to show the huge range of conductivities displayed by the Si–Ge system; at 150 K, the data span a factor of $\sim$1000 in conductivity.

The thermal conductivity of our Si–Ge superlattice samples falls below the conductivity of SiGe alloys and above the conductivity of *a*-Si (see Fig. 2). All films show similar temperature dependence: the conductivity is approximately constant at $T>200$ K and decreases gradually with decreasing temperature for $T<150$ K. We see that the highest conductivity film has an intermediate superlattice period L and films with $L>130$ Å have the lowest conductivity.

In Fig. 3, we plot the conductivity at $T=200$ K as a function of L to show this dependence more clearly. We compare our results to the through-thickness thermal conductivity of (AlAs)–(GaAs) superlattices from Ref. 7. The number of data points is limited but we can conclude that the conductivity of Si–Ge superlattices is always smaller than (AlAs)–(GaAs); and that the conductivity of short-period samples ($L<70$ Å) shows a significant suppression with decreasing L. For long-period samples ($L>130$ Å), the conductivity is small and nearly independent of L. This decrease in conductivity for large L is not observed in the thermal conductivity of (AlAs)–(GaAs) superlattices.[4]

We first discuss the data for short-period ($L<70$ Å) Si–Ge superlattices. Quantitative modeling of heat transport in superlattice materials is a complex task that is beyond the scope of this work: the effects of superlattice structure on the vibrational mode energies, dispersions, and lifetimes are not well known. But we can set a lower limit to the thermal conductance of the interfaces G using $\Lambda = GL/2$, where Λ is the thermal conductivity of the shortest period sample; $G \approx 2\times 10^9$ W m^{-2} K^{-1} at 200 K (see Fig. 3). The true value of the interface conductance G will be larger than this lower limit because of the finite thermal conductivity of the individual Si and Ge layers. We note that the largest thermal conductance ever observed for an individual solid–solid interface, Ti/Al_2O_3, is a factor of 10 smaller, $G \approx 2\times 10^8$ W m^{-2} K^{-1}.[18]

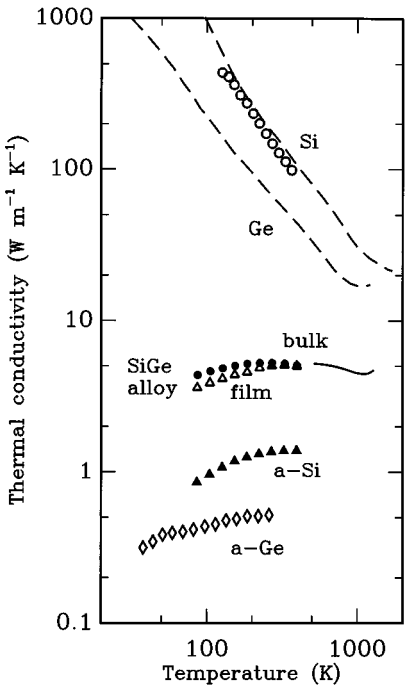

FIG. 1. Thermal conductivity of bulk SiGe alloy (filled circles) and thin film SiGe alloy (open triangles) with comparison to data for the pure crystals and the amorphous phases. The compositions of the bulk and thin film alloy are $Si_{0.8}Ge_{0.2}$ and $Si_{0.85}Ge_{0.15}$, respectively. Data points for $80<T<400$ K, are acquired using the 3ω method; high temperature data ($T>500$ K) for the SiGe bulk alloy (Ref. 15) were provided by C. B. Vining, private communication. Dashed lines are for single crystal Ge and Si from Ref. 16. Data for *a*-Si and *a*-Ge are from Refs. 13 and 17, respectively.

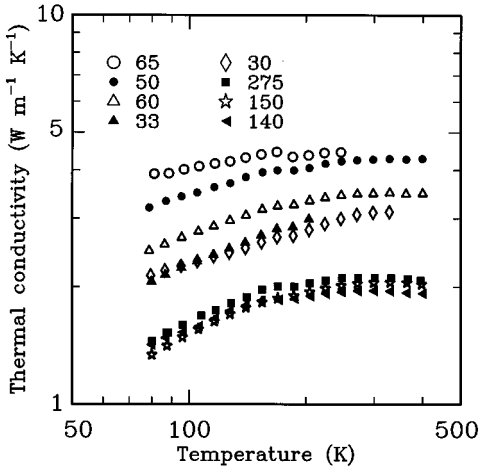

FIG. 2. Thermal conductivity of Si–Ge superlattices. Each symbol is labelled by the superlattice period L measured in Å.

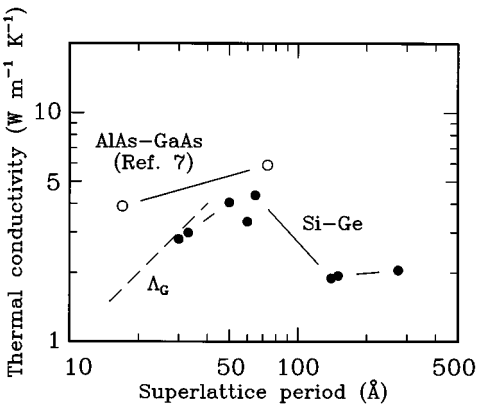

FIG. 3. Thermal conductivity of Si–Ge superlattices (filled circles) at $T=200$ K plotted as a function of superlattice period L. The lines are to ''guide-the-eyes.'' Open circles are data for (AlAs)–(GaAs) superlattices from Ref. 7. The dashed line shows the behavior expected if the conductivity is dominated by the thermal conductance of the interfaces G with $G\approx 2\times 10^9$ W m^{-2} K^{-1}.

We compare these estimates of G to the predictions of the diffuse-mismatch model (DMM);[10] the DMM assumes that all incident phonons scatter randomly but elastically at the interface. (For many combinations of materials, the predictions of the more complex acoustic-mismatch model are essentially the same as the DMM.) The DMM predicts a thermal conductance for Si–Ge interfaces that is a factor of 3 smaller than our experimental lower limit at room temperature. The discrepancy at 80 K increases to a factor of 8. Thus, we conclude that the assumptions of the DMM are poorly satisfied at epitaxial Si–Ge interfaces. This conclusion is even more striking when we note that the DMM is often observed to *overestimate* the room temperature thermal conductance of single metal–dielectric interfaces.[10,18] Thus, lower thermal conductivity superlattices may be possible if a way can be found to reduce the thermal conductance of SiGe interfaces to the lower values predicted by the DMM.

Finally, we turn our attention to the very low thermal conductivity observed in films with $L>130$ Å (see Figs. 2 and 3). Clearly, the Si–Ge interfaces cannot explain this behavior. Instead, we argue that the relatively poor crystal quality of these long-period superlattices is responsible for the strong reduction in conductivity.

Assume for the sake of this argument that a Si–Ge superlattice is grown with equal layer thickness of Si and Ge, and that the average lattice constant of the film has relaxed to a point halfway between the lattice constant of Si and Ge. For short-period superlattices, we expect the individual layers to be fully strained: 2% tensile strain for Si and 2% compressive strain for Ge. But when the individual layer thicknesses exceed the critical thickness for the formation of dislocations, the layers will partially relax with the creation of a high density of extended defects.[19] The critical thickness for 2% compressively strained Ge(001) is $h_c\simeq 60$ Å but for Si(001), with 2% tensile strain, h_c is only $\simeq 30$ Å.[20] Thus, we believe that for superlattices with $L>130$ Å, the Si layers have greatly exceeded h_c and the growth of each Si or Ge layer introduces a large density of dislocations and stacking faults. The surprising observation is that this plastically deformed Si–Ge material exhibits a thermal conductivity that approaches the low values characteristic of amorphous solids.[11]

This work was supported by National Science Foundation Grant No. CTS-9421089. Samples were grown at the Research Triangle Institute. Sample characterization by RBS and XRD was carried out in the Center for Microanalysis of Materials, University of Illinois, which is supported by the U.S. Department of Energy under Grant No. DEFG02-91-ER45439. The authors thank Cronin Vining for providing a sample of well-characterized, sintered SiGe alloy.

[1] L. D. Hicks, T. C. Harman, and M. S. Dresselhous, Appl. Phys. Lett. **63**, 3230 (1993).
[2] R. Venkatasubramanian, T. Colpitts, E. Watko, and J. Hutchby, Proceedings of 15th International Conference on Thermoelectrics (IEEE, Piscataway, NJ, 1996), catalog No. 96TH8169, pp. 454–458.
[3] C. L. Tien and G. Chen, J. Heat Transfer **116**, 799 (1994).
[4] T. Yao, Appl. Phys. Lett. **51**, 1798 (1987).
[5] G. Chen, C. L. Tien, X. Wu, and J. S. Smith, J. Heat Transfer **116**, 325 (1994).
[6] X. Y. Yu, G. Chen, A. Verma, andJ. S. Smith Appl. Phys. Lett. **67**, 3554 (1995).
[7] W. S. Capinski and H. J. Maris, Physica B **219&220**, 699 (1996).
[8] V. Narayamurti, H. L. Stormer, M. A. Chin, A. C. Gossard, and W. Wiegmann, Phys. Rev. Lett. **43**, 2012 (1979).
[9] C. Colvard, T. A. Gant, M. V. Klein, R. Merlin, R. Fisher, H. Morkoc, and A. C. Gossard, Phys. Rev. B **31**, 2080 (1985).
[10] E. T. Swartz and R. O. Pohl, Rev. Mod. Phys. **61**, 605 (1989).
[11] David G. Cahill, S. K. Watson, and R. O. Pohl, Phys. Rev. B **46**, 6131 (1992).
[12] J. P. Dismukes, L. Ekstrom, E. F. Steigmeir, I. Kudman, and D. S. Beers, J. Appl. Phys. **35**, 2899 (1964).
[13] David G. Cahill, M. Katiyar, and J. R. Abelson, Phys. Rev. B **50**, 6077 (1994).
[14] S.-M. Lee and D. G. Cahill, J. Appl. Phys. **81**, 2590 (1997).
[15] C. B. Vining, William Laskow, Jack O. Hanson, Roland R. Van der Beck, and Paul D. Gorsuch, J. Appl. Phys. **69**, 4333 (1991); see description of sample No. 131.
[16] C. J. Glassbrenner and G. A. Slack, Phys. Rev. **134**, A1058 (1964).
[17] D. G. Cahill and R. O. Pohl, Phys. Rev. B **37**, 8773 (1988).
[18] R. J. Stoner and H. J. Maris, Phys. Rev. B **48**, 16373 (1993).
[19] J. W. Matthews and A. E. Blakeslee, J. Cryst. Growth **27**, 118 (1974).
[20] J. E. Van Nostrand, David G. Cahill, I. Petrov, and J. E. Greene (unpublished).